INELASTIC ANALYSIS OF STEEL BRACED FRAMES WITH FLEXIBLE JOINTS

W. F. CHEN

School of Civil Engineering, Purdue University, West Lafayette, IN 47907, U.S.A.

and

S. P. ZHOU

Chongqing Institute of Communication, Chongqing, Sichuan, China

Abstract—Conventional analysis and design of steel frameworks is usually carried out under the assumption that the connections joining the beams to the columns are either fully rigid or ideally pinned. Recently, the non-linear behavior of connecting joints has received an explicit consideration in the new AISC/LRFD Specification. This paper focuses on the study of the true non-linear behavior of in-plane braced frames using a more refined method for inelastic analysis, considering the influence of flexible joints and the loading pattern on the behavior and strength of such frames. To this end, extensive numerical studies are made using the computer model developed. The influences of connection flexibility on moment transfer mechanism between the beams and the columns, the load carrying capacity and deformational behavior, and the failure modes of these frames are described.

1. INTRODUCTION

Conventional structural analysis of frames is usually carried out by one of the following methods of analysis with the usual assumptions that the connections joining the beams and columns are either fully rigid or pinned:

- (a) first-order elastic analysis;
- (b) second-order elastic analysis;
- (c) first-order, rigid–plastic analysis;
- (d) second-order, rigid–plastic analysis;
- (e) second-order, elastic–plastic hinge analysis.

All these methods are approximate in nature because of the major assumptions of elasticity and rigid–plasticity for the non-linear behavior of the material. Further, the non-linear behavior of connecting joints has recently received an explicit consideration in the new AISC/LRFD Specification[1]. The work described in this paper focuses on the true non-linear behavior of in-plane braced frames using a more refined method for inelastic analysis, considering the influence of flexible joints and the loading pattern on the behavior and strength of such frames.

2. SYSTEM ANALYZED

2.1. *The frames*

The type and size of braced frames analyzed here are shown in Fig. 1. In the Type A frame, the slenderness ratio of the columns is $L_c/r_x = 40.3$ and the relative stiffness between the beam and column is taken to be $G_b/G_c = (EI_b/L_b)/(EI_c/L_c) = 8.18$. In the Type B frame, we take the same column slenderness ratio of Type A ($L_c/r_x = 40.3$), but with a different stiffness ratio $G_b/G_c = 4.0$. In the Type C frame, we choose $L_c/r_x = 60.5$ and $G_b/G_c = 4.0$. Here, L is the length of the member, r_x the radius of gyration of the cross-section about the strong bending axis, E the elastic modulus, I the moment of inertia of the section, and subscripts c and b denote column and beam, respectively. All beams and columns in the
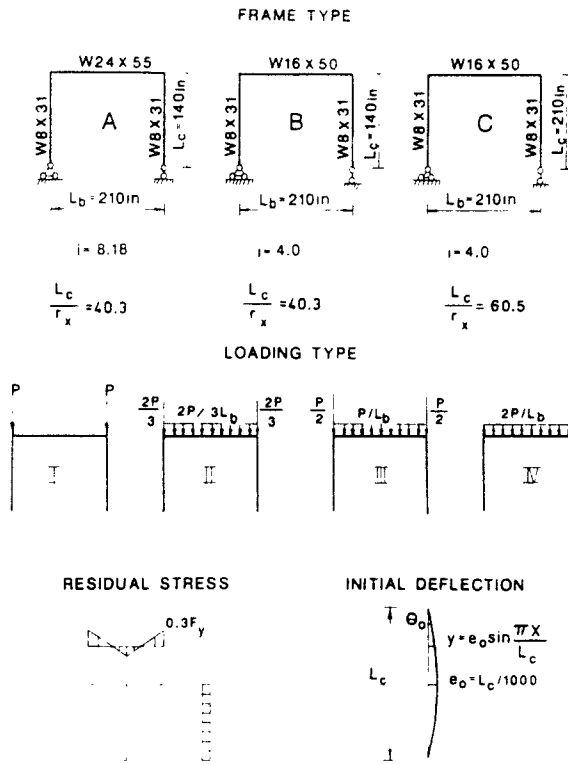
Fig. 1. Frame type, loading pattern, residual stress, and initial deflection $(i = G_b/G_c)$.

three types of frames are connected about their strong axis bending direction. The buckling of these frames will occur in the weak-axis plane bent about the strong axis. The 3-D out-of-plane buckling is not considered in this study.

2.2. The imperfections

The same residual stress distribution as shown in Fig. 1 is used for both columns and beams. The initial out of straightness of all columns is taken to be $L_c/1000$ (Fig. 1).

The steel is assumed to be an elastic–perfectly plastic material and the influence of elastic unloading from a plastic state is neglected.

2.3. The loading patterns

Four types of loading patterns are considered.

Type I—all loads are applied on the top of columns.

Type II—one third of the total load is distributed uniformly along the beam and two thirds is on the column tops. In this case, the columns are loaded with a small eccentricity.

Type III—half of the total load is distributed uniformly over the beam and the other half is on the column tops. In this case, the columns are loaded with a medium eccentricity.

Type IV—all loads are applied on the beam, so the columns are loaded with a rather large eccentricity.

2.4. The flexible connections

In real frames, the rotational stiffness of connections joining the beams and columns is neither infinite nor zero. The relationship between moment, M_r, and rotation, θ_r, for a semi-rigid connection is nonlinear and depends on the detailing of a given joint. In this paper, four types of M_r–θ_r curves are considered.
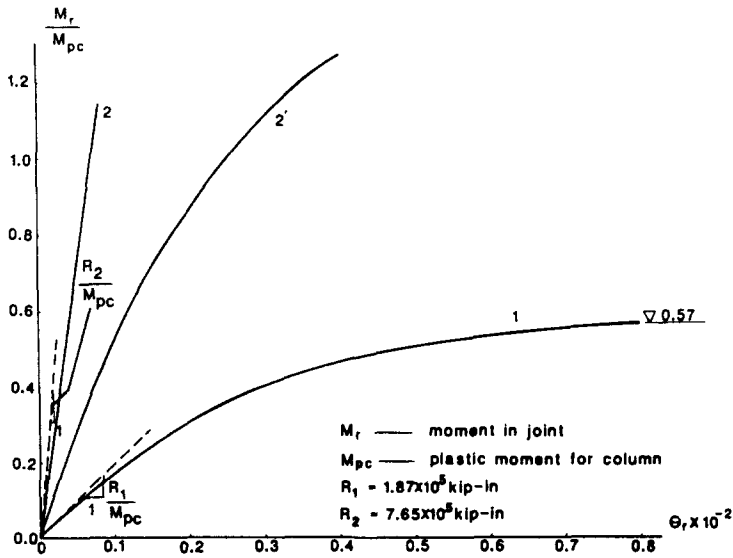
Fig. 2. The moment and rotation curves of semi-rigid joints.

Type 0 is for pinned connections.
Type 3 is for rigid connections.
Types 1 and 2 as shown in Fig. 2 are for semi-rigid flexible connections.

To model the behavior of the semi-rigid connections, we use the exponential function proposed by Lui[2]

$$M_r = \sum_1^6 C_j(1 - e^{-\theta_r/2j\alpha})$$ (1)

where α is the scaling factor and C_j parameters.

The moment rotation behavior of flexible connections can also be represented by the polynomial model proposed by Frey and Morris[3] or the B-spline curve-fitting technique proposed by Jones et al.[4], among others. However, there are major drawbacks in these models. Since the nature of a polynomial is to peak and trough within a certain range, the stiffness of the connection (as represented by the first derivative of the polynomial) may be negative which is physically unjustifiable. To overcome this, Jones et al.[4] used a cubic B-spline curve-fitting technique to improve the polynomial model. In the cubic B-spline model, a cubic polynomial is used to fit segments of a curve. Continuity between the first, and second derivatives of each segment of the curve are enforced. Although the cubic B-spline model gives a good representation of the connection behavior and circumvents the problem of negative stiffness, large number of data are necessary for the curve-fitting process. To overcome this, the exponential model proposed by Lui[2] is used here.

The values of α and C_j in eqn (1) for Type 1 and Type 2 flexible connections are listed in Table 1. R_1 and R_2 are their initial stiffnesses as defined in Fig. 2 and their values are also listed in Table 1.

The maximum moment capacity of a connection is called the connection limiting moment. For Type 3 and Type 2 connections, the connection limiting moment is designed to be greater than that of the full plastic moment capacity of the column M_{pc}, but for Type 1 connection it is equal to $0.57M_{pc}$.

The moment–rotation curve for Type 2' connection as shown in Fig. 2, lies somewhere between Type 1 and Type 2 curves. Frame analysis results with Type 2' connections are found very close to those with Type 2 connections and are therefore omitted from the following discussion.

In the following, we shall present the frame analysis for different load patterns and

Table 1. Parameters for connection

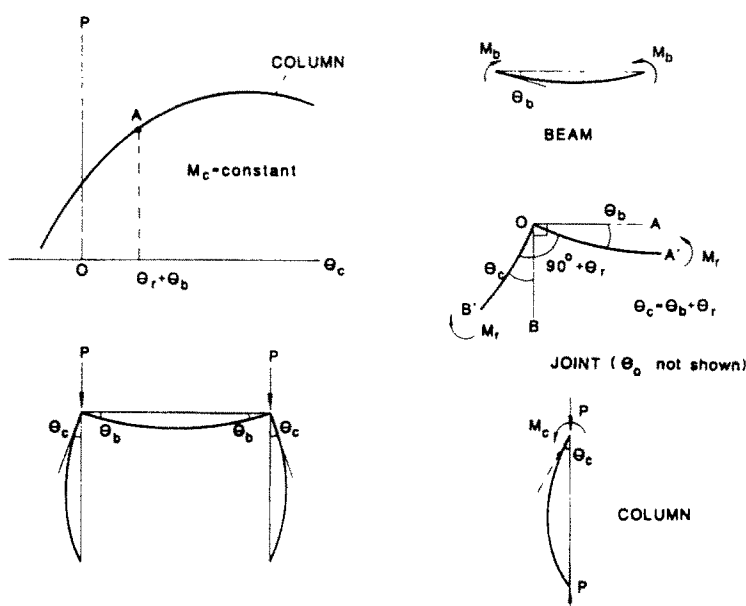|	Type 1	Type 2
C_1	-0.37565×10^2	-0.39543×10^3
C_2	0.10758×10^4	0.12055×10^5
C_3	-0.77282×10^4	-0.10161×10^6
C_4	0.22126×10^5	0.32710×10^6
C_5	-0.28368×10^5	-0.43511×10^6
C_6	0.13544×10^5	0.20147×10^6
α	0.10789×10^{-3}	0.66828×10^{-4}
R_i	1.87×10^5 kip-in	7.65×10^5 kip-in

Fig. 3. Calculation of Type B and C frames with loads on columns only (Type I loading).

connection types. The method of analysis is rigorous and inelastic. For comparison, some typical results from second-order elastic analysis and eigenvalue analysis are also given in the forthcoming section.

3. ELASTIC EIGENVALUE ANALYSIS (FRAMES B AND C, LOADING TYPE I)

For Type B and C frames with loads on columns only (Type I loading) as shown in Fig. 3, we first neglect the initial out of straightness of the columns and take Type 1 and Type 2 connections as linear elastic joints with constant stiffnesses R_1 and R_2 (Fig. 2) for the eigenvalue analysis of Frame B-I-3,2,1 (Frame B—Loading Type I—Connection Type 3, 2, 1, as shown in Fig. 1) and Frame C-I-3,2,1. When the axial load P on the top of the two columns reaches the critical load P_{cr}^F, the frame will be in a neutral equilibrium condition. Based on the deformed configuration shown in Fig. 3, the P_{cr}^F can be derived in a rather straightforward manner. This is briefly summarized in the following in order to introduce the notations and sign conventions used for subsequent discussions.

The beam bends downward (or upward). The moment M_b induced in the beam is uniform and the end rotation θ_b is given by

$$\theta_b = \frac{M_b}{2G_b}. \tag{2}$$

The two columns in the frame will bend outward (or inward) but the end moment M_c and end rotation θ_c have opposite directions, so there exists an inflection point in the

column. Using the slope-deflection equation of the beam-column, the end rotation for the column has the value

$$\theta_c = \frac{M_c}{G_c(kL_c)^2}\left[1 - kL_c \frac{\cos kL_c}{\sin kL_c}\right] \tag{3}$$

where

$$k = \sqrt{\left(\frac{P_{cr}^F}{EI_c}\right)}.$$

The angle at the joint between the beam and the column will open up and enlarge by an amount θ_r. For a linear elastic moment and rotation relation, θ_r has the value

$$\theta_r = \frac{M_r}{R_i} \tag{4}$$

where R_i denotes R_1 or R_2 for connection Type 1 or Type 2, respectively, as shown in Fig. 2 and $R_i = R_3 = \infty$ for rigid connections (Type 3).

To satisfy the compatibility and equilibrium conditions at the joint, the following relations must hold:

$$\theta_c = \theta_b + \theta_r \tag{5a}$$

$$M_b = -M_c \tag{5b}$$

$$M_b = -M_c = M_r. \tag{5c}$$

In eqns (2)-(5), moment and rotation for the beam and the column are positive if they are in the clockwise direction but M_r and θ_r are positive if they tend to open up the joint.

Combining eqns (2)-(5), we have

$$\frac{M_r}{R_i} + \frac{M_b}{2G_b} = \frac{M_c}{G_c(kL_c)^2}\left[1 - kL_c \frac{\cos kL_c}{\sin kL_c}\right]. \tag{6}$$

Rearranging, we obtain the characteristic equation for eigenvalues

$$\frac{G_c}{2G_b}\left[1 + \frac{2G_b}{R_i}\right](kL_c)^2 - kL_c \frac{\cos kL_c}{\sin kL_c} + 1 = 0 \tag{7}$$

where

$$G_c = \frac{EI_c}{L_c}$$

$$G_b = \frac{EI_b}{L_b}.$$

Table 2. K_c and K_p in Frames B-I and C-I

Connection type	K_c		K_p	
	B-I	C-I	B-I	C-I
1	0.819	0.790	0.714	0.742
2	0.786	0.762	0.714	0.742
3	0.772	0.751	0.714	0.742

For Frames B-I-3,2,1 and C-I-3,2,1, we solve eqn (7) using Broyden's method with the aid of a computer and obtain the critical value of (kL_c) from which the critical load P_{cr}^F is

$$P_{cr}^F = \left[\frac{(kL_c)}{L_c}\right]^2 EI_c. \tag{8}$$

Comparing P_{cr}^F with Euler load $P_{cr} = \pi^2 EI_c/L_c^2$ for columns in Frame B-I-0 or Frame C-I-0 (i.e. pinned-end frame), the effective length factor K_c can be determined as

$$K_c = \sqrt{\left(\frac{P_{cr}}{P_{cr}^F}\right)} = \frac{\pi}{kL_c}. \tag{9}$$

The effective length factor K_c is a measure of the end restraint of the column provided by the beam and the joint.

The values of K_c for Frames B-I-3,2,1 and C-I-3,2,1 are summarized in Table 2. From this table, we can see that the K_c for Frame B is larger than that for Frame C, and K_c for a weaker joint is larger than that for a stiffer one.

4. INELASTIC ANALYSIS WITHOUT LOADS ON BEAM (FRAMES B AND C, LOADING TYPE I)

For the inelastic analysis of Frames B-I and C-I, the equilibrium and compatibility conditions (eqn (5)) and the M_b vs θ_b relation for the beam (eqn (2)) remain the same because the moment in the beam is generally small and will remain in the elastic range during the complete loading process of Frames B-I and C-I. However, the $M_r-\theta_r$ relations for Type 1 and Type 2 connections are nonlinear and eqn (1) must be used here.

The exact inelastic analysis for imperfect columns in Frames B-I and C-I is a rather complicated task and it was carried out by a computer program developed at Purdue University. The column in this program is assumed to be imperfect with residual stress and initial deflection as shown in Fig. 1. In the analysis, the column is loaded first with a constant moment M_c on the top in the opposite direction to that of the initial deflection. The column is divided into eight segments. As the axial force P is increased incrementally, compatibility conditions are enforced at each division point. For a selected value of M_c, the $P-\theta_c$ curve can be traced for the column from the program (Fig. 3). From eqns (5b) and (5c), the values of M_b and M_r are determined from the given value of M_c, and the corresponding values of $|\theta_r|$ and θ_b are then derived from eqns (1) and (2). With $\theta_c = \theta_b + \theta_r$ (eqn (5a)), Point A on the $P-\theta_c$ curve (with M_c = constant) can be located. The set of values P, M_c, θ_c, θ_b and θ_r so obtained corresponding to Point A, represents the solution of this imperfect frame at the axial load level P. Taking different values of M_c, a complete load–rotation $(P-\theta_c)$ curve for the frame can be traced.

Figures 4 and 5 show such a set of curves of (M_c/M_{pc}) vs θ_c, and (M_c/M_{pc}) vs (P/P_y) for Frames B-I-3,2,1 and C-I-3,2,1. Here, M_{pc} is the plastic moment capacity of the column section, P_y is its yield load. As the load P/P_y increases to its peak value, the curve approaches the horizontal line. The maximum load-carrying capacity for Frame B-I is $P/P_y = 0.951$ and for Frame C-I is 0.9. Further loading beyond the peak load will result
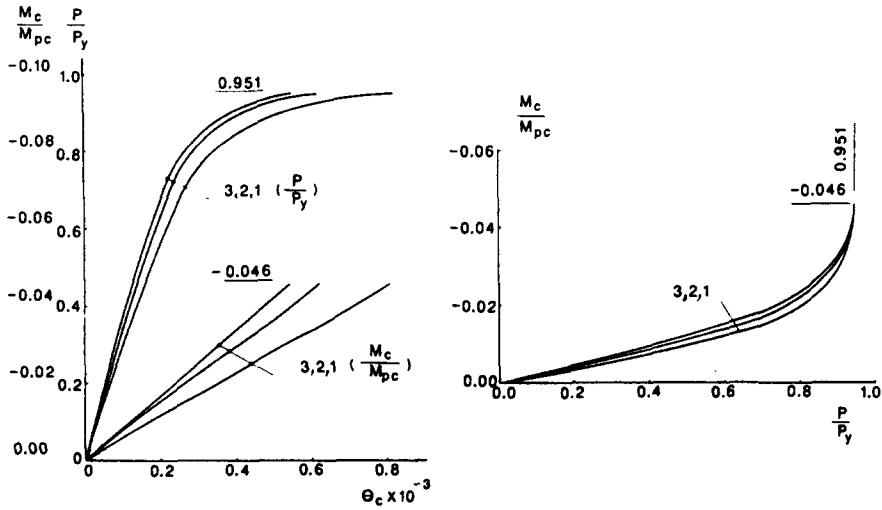
Fig. 4. The force, moment and rotation of frame B under Loading Type I with Connection Type 1, 2 and 3 (B-I-1,2,3).
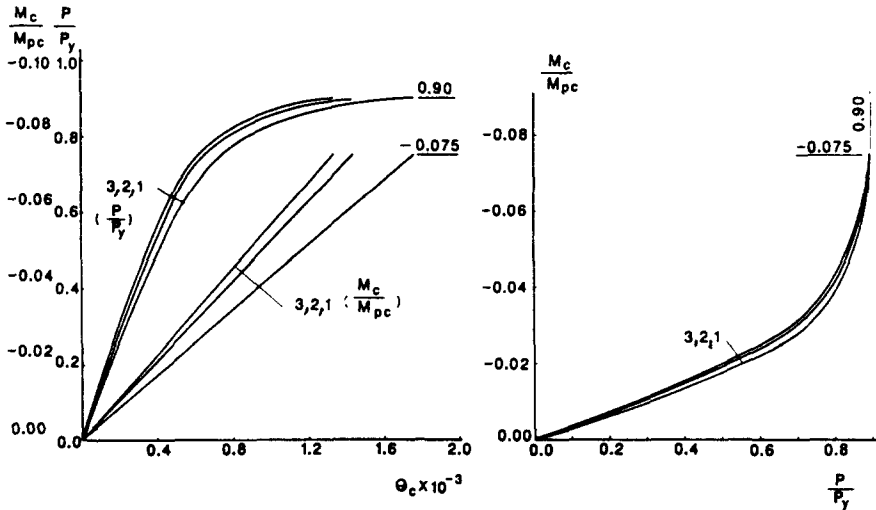

Fig. 5. The force, moment and rotation in Frame C under Loading Type I with Connection Type 1, 2 and 3 (C-I-1,2,3).

in a descending branch of the curve. This is not attempted here.

The (M_c/M_{pc}) vs θ_c curves shown in Figs 4 and 5 are almost linear and the maximum value of M_c/M_{pc} is very small (-0.046 and -0.075) as the axial load P/P_y increases.

The relationship between M_c/M_{pc} and P/P_y is nearly linear up to $P/P_y = 0.8$ and 0.7 but becomes nonlinear and the slope increases rapidly when the axial load P/P_y approaches its maximum value. The slope of the curve is vertical at the peak load $P/P_y = 0.951$ and 0.9. Beyond the peak point, the M_c/M_{pc} value will continue to increase as the axial load P/P_y decreases along its descending branch. This is because, at this stage of loading, the second-order moment is very large and it requires a large opposite end moment to balance it.

For different types of connections (Types 1–3), the maximum load-carrying capacity $P/P_y = 0.951$ and 0.9 for the two frames is the same except that the deformations of the frames with flexible connections are greater than that of rigid ones. This is because during the entire loading process, the joint moment M_r remains very small and the M_r vs θ_r relation is almost linear at this moment level.

If the end restraint of the column provided by the connection is very small, the maximum load P/P_y of the frame will decrease to the maximum load-carrying capacity of

a centrally loaded column with pinned ends. The maximum loads for this extreme case are $P/P_y = 0.917$ for Frame B and 0.837 for Frame C. This will be described later (see Fig. 12).

Using the computer program and taking $M_c = 0$ (i.e. a centrally loaded column case) it was found that L_c/r_x has to be 28.78, for the maximum load $P/P_y = 0.951$ for Frame B-I and $L_c/r_x = 44.9$ for the maximum load $P/P_y = 0.90$ for Frame C-I. The plastic effective length factor for Frame B-I has the value $K_p = 28.78/40.3 = 0.714$ and for Frame C-I, it has the value $K_p = 44.9/60.5 = 0.742$. The value of K_p for Frame B-I is smaller than that in Frame C-I, but both K_p values are smaller than the corresponding K_e values (Table 2). This is because in the inelastic analysis, the beam remains in the elastic range, the joint is almost in the elastic range, but the column is in the plastic range. As a result, the G_b/G_c ratio increases in this range and so do the relative end restraints of the beam and the joints to the columns. The column in Frame B is shorter than that in Frame C, so the plastic range for columns in Frame B is greater than that in Frame C, i.e. the G_b/G_c in Frame B is greater than that in Frame C. We can therefore assume that, using the elastic K_e to replace the plastic K_p for frames with loads acting on the tops of columns will provide a convenient and conservative value for columns in real frames.

5. SECOND-ORDER ELASTIC ANALYSIS FOR FRAMES WITH LOAD ON BEAM (FRAME B, LOADING TYPE III)

In the second-order elastic analysis for the frame (Type B) with loads on the beam and columns (Type III) as shown in Fig. 6, the initial deflection of columns is neglected and the connection Types 1 and 2 will be treated as linear elastic joints with constant rotational stiffnesses R_1 and R_2, respectively, as in the eigenvalue analysis (Section 3). Under an increasing load, the frame will deform as shown in Fig. 6.

The beam bends downward. The end moment M_b and the end rotation θ_b are related by

$$\theta_b = \frac{M_b + qL_b^2/12}{2G_b} \tag{10}$$

where q is the uniformly distributed load on the beam, $q = P/L_b$, and P is the axial force on the column.

Using the compatibility condition (5a) and the moment–rotation relation (4) at the joint, we have

$$\theta_c = \theta_b - \frac{M_c}{R_i}. \tag{11}$$

Substituting eqns (3) and (10) into eqn (11) and using eqn (5b), we obtain

$$M_c = \frac{\frac{1}{12}qL_b^2}{\left(\frac{2G_b}{G_c}\right)\frac{1}{(kL_c)^2}\left[1 - kL_c\frac{\cos kL_c}{\sin kL_c}\right] + 1 + \frac{2G_b}{R_i}}. \tag{12}$$

Equations (12), (10), and (3) describe the behavior of the frame with loads on the beam and the columns. When the denominator in eqn (12) approaches zero, the values of M_c and θ_c will approach infinity and the corresponding load P is the maximum load-carrying capacity of the elastic frame. This condition is identical to that of the eigenvalue equation (7). Here, as in the eigenvalue analysis, the maximum load-carrying capacity of the elastic frame with lateral loads is the corresponding eigenvalue load.

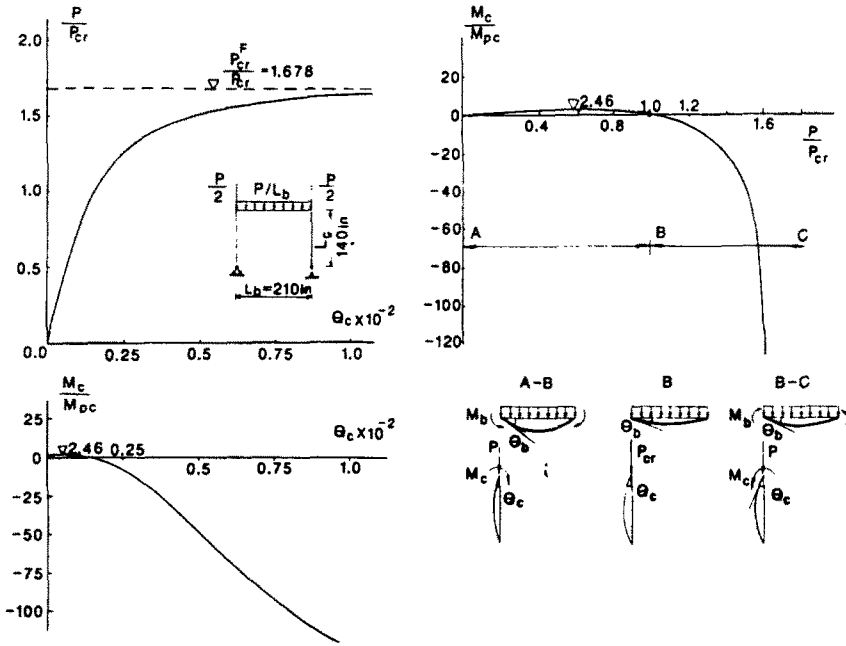With eqns (12) and (3) we can now construct the (P/P_{cr}) vs θ_c curve, and the (M_c/M_{pc})

Fig. 6. Second-order elastic analysis of rigid Frame B with loads on beam and columns (Type III) (B-III-3).

vs (P/P_{cr}) curve for Frame B-III-3 as shown in Fig. 6. For the (P/P_{cr}) vs θ_c curve, the angle θ_c increases slowly with P/P_{cr} until the value $P = P_{cr}$ is reached. As P increases beyond this limit, the curve bends over rapidly and approaches zero slope as P/P_{cr} approaches its maximum value $P_{cr}^F/P_{cr} = 1.678$.

As for the curve (M_c/M_{pc}) vs θ_c, the angle θ_c increases slowly as M_c/M_{pc} increases to its peak value 2.46, then M_c/M_{pc} decreases and finally becomes negative as θ_c increases. At the limit when θ_c approaches infinity, the M_c/M_{pc} approaches negative infinity.

The interaction between M_c/M_{pc} and P/P_{cr} can best be illustrated by the curve shown in Fig. 6. This curve has two parts A–B and B–C. In part A–B, the end moment M_c acts in the same direction as the end rotation θ_c, while the end moment M_b on the beam is in the opposite direction to that of θ_b. The beam bends downward with an opposite end moment that produces an inflection point in the beam. This implies that in the loading range A–B, the beam gets help from the column to carry an extra load through the restraint provided by the column. The restraint moment increases initially from zero to its maximum value 2.46 and then drops down to zero again. At Point B, M_c/M_{pc} is zero and $P/P_{cr} = 1$, i.e. the column now behaves as a centrally loaded column with pinned ends, and provides no restraint to the beam at this load level. The column and beam are essentially independent of each other at this load level, even though they are connected by a joint.

In region B–C (θ_c and M_c/M_{pc} can be infinity at C), the situation is reversed. Here, M_c and θ_c act in the opposite directions but M_b and θ_b act in the same direction since M_c is negative and M_b is positive. As P increases, the second-order moment in the column becomes very large. To maintain compatibility at the joint, the beam must now provide restraint to the column and to help the column to carry an extra load until P/P_{cr} reaches the limit load P_{cr}^F/P_{cr} at which M_c/M_{pc} approaches infinity.

The behavior of frames with flexible connections (Types 1 and 2) is not shown in Fig. 6. From eqn (12), it can be seen that the more flexible the connection is (i.e. the less the R_i is), the less the M_c will be. This implies that the flexibility of a connection will reduce the restraint capacity between the beam and the column. As a result, the maximum load-carrying capacity of the frame will be reduced for the second-order elastic analysis.
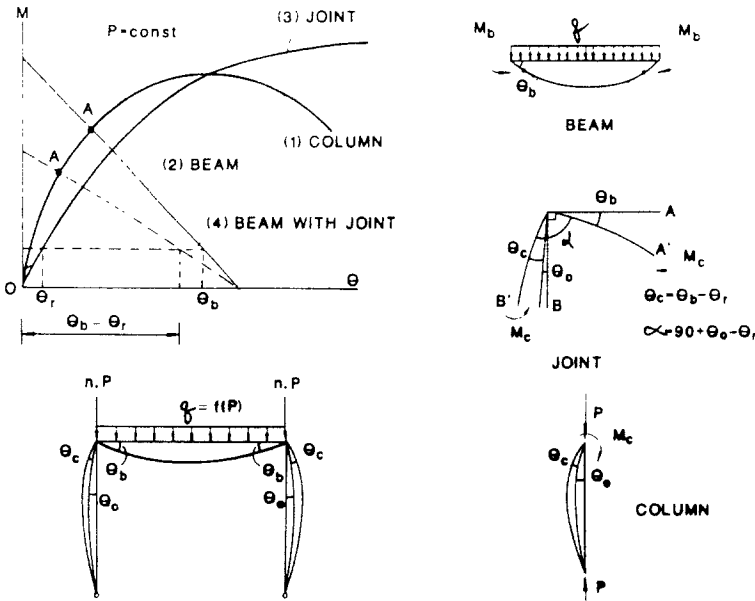
Fig. 7. Inelastic analysis for frames with load on beam.

6. INELASTIC ANALYSIS FOR FRAMES WITH LOAD ON BEAM (FRAMES A AND B—LOAD TYPES II–IV)

6.1. Method of analysis

When the maximum load is reached in Frame A or B, Loading Types II, III, or IV, the columns will always be in the inelastic range but the beam may be in the inelastic range or may still remain in the elastic range depending on the peak load level. To solve this problem, a computer program developed previously by Zhou and Chen[5] is used here. In the present analysis, the beam is divided into 24 segments. Using the tangent stiffness method reported by Chen and Atsuta[6], the curvature at each division point can be calculated from the known lateral load and end moments. Assuming that the curvature varies linearly within the segment, the deflection at each division point can be computed by Newmark's numerical integration method from which the end rotation can be calculated. For a given value of P, the lateral load distribution q on the beam is known (Fig. 1). Using the computer program, this dependence of the end moment M_b on the end rotation θ_b can be determined. This relationship is marked as beam curve (2) in the $M-\theta$ coordinate system in Fig. 7. If the load is small, curve (2) will be linear, otherwise, it will be nonlinear.

Using the computer program, the end moment–rotation curve $(M_c-\theta_c)$ for the columns with constant axial force P can also be traced as the curve marked (1) in Fig. 7. For the rigid connection (Type 3), we have $\theta_b = \theta_c$, it follows that the intersection Point A of curves (1) and (2) is the solution point for the frame with a rigid connection.

For a flexible connection (Types 1 and 2), eqn (5a) must be used. Since M_c is positive in the inelastic analysis, curve (4) in Fig. 7 can be obtained by subtracting curve (3) from curve (2) where curve (3) is the $M_r-\theta_r$ curve for the connection used at the joint. This procedure is coded in the computer program. The intersecting point A' of curve (1) with curve (4) in Fig. 7 gives the solution for a frame with a flexible connection.

By varying the total force P, a series of curves (1), (2) and (4) can be constructed. From these curves a series of Points A or A' can be generated so that the complete response of an inelastic, imperfect frame with flexible joints can be described. Details of this procedure with rigid connections can be found in the books by Chen and Atsuta[6] and Galambos[7].

6.2. Frame with small eccentricity in columns

Figure 8 shows the process of calculations made for Frame A with Load Pattern II and Connection Type 3. In this case, the columns are subjected to a relatively small end moment from the beam because the beam has to carry only one-third of the total applied
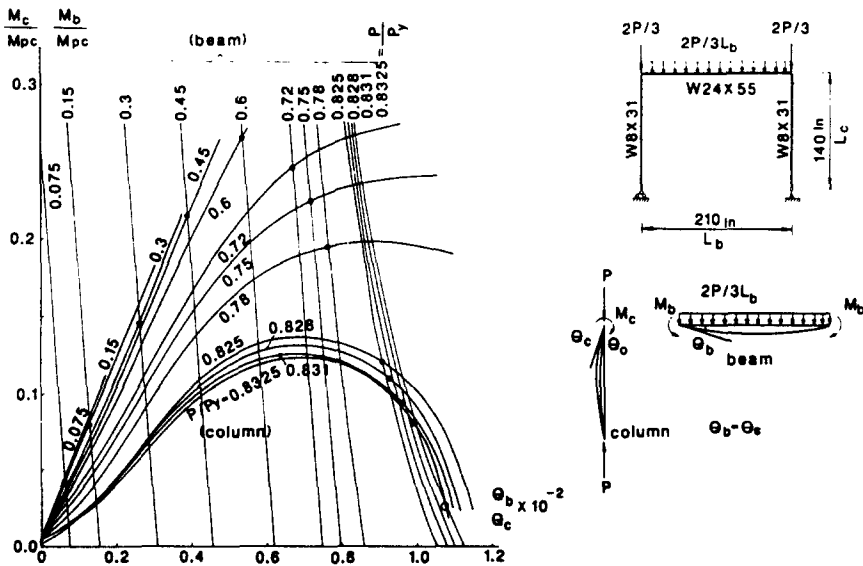
Fig. 8. The process of calculations for the $(M/M_{pc})-\theta$ curve of the rigid frame (A-II-3).

load. In Fig. 8, we choose $P/P_y = 0.075, 0.15, 0.3, 0.45, 0.6, 0.72, 0.75, 0.78, 0.825, 0.828, 0.831, 0.8325$. The $M-\theta$ curves for the column and for the beam are plotted and the corresponding intersecting points are traced and marked using the condition $\theta_b = \theta_c$ for rigid connection. When $P/P_y = 0.834$, the curves for the beam and for the column do not intersect. This implies that the frame cannot carry this load. When $P/P_y = 0.8325$, the curves for the beam and for the column intersect each other twice: the first intersection point is marked with a solid circle and the second with an open circle on the curve. The maximum load P/P_y for the frame lies somewhere between the values 0.8325 and 0.834. At the peak load, the corresponding beam curve and the column curve will be tangent to each other at a single point. This peak point lies somewhere between the solid and open circles for the $P/P_y = 0.8325$ curve. Thus, all the solid circles lie on the ascending branch of the load–rotation curve $(P/P_y$ vs $\theta_c)$ of the frame, while all the open circle points are on the descending branch of the curve. Since the convergence becomes difficult in the numerical analysis involving the descending branch of the load–rotation curve of the frame, only a few points are made in the present calculation.

For the flexible connections (Types 1 and 2), the procedure is almost identical to the rigid case except that the compatibility condition $\theta_c = \theta_b - \theta_r$ is used.

Figure 9 shows the curves of (P/P_y) vs θ_c, (M_c/M_{pc}) vs θ_c, (M_c/M_{pc}) vs (P/P_y) and (M_{bo}/M_{pb}) vs (P/P_y) for Frame A with Loading Pattern II—Connection Type 1, 2, 3. Here M_{bo} is the moment at the midspan of the beam and M_{pb} is the full plastic moment capacity of the beam.

In Fig. 9, the load–rotation curve (P/P_y) vs θ_c has an ascending and a descending branch. The peak point of the curve is the maximum load-carrying capacity of the frame. The maximum load P/P_y is about 0.833.

In the (M_c/M_{pc}) vs θ_c curve, as θ_c increases, M_c increases almost linearly up to its maximum value (0.265, 0.25, 0.215 for Connection Type 3, 2, 1, respectively). After the peak value, M_c decreases while P/P_y continuously increases with increasing θ_c. In the descending branch of the (P/P_y) vs θ_c curve, the M_c value continuously drops and becomes negative for a very large end rotation θ_c.

In the (M_c/M_{pc}) vs (P/P_y) curve, as load P/P_y increases, the column moment M_c increases first until the maximum value of M_c/M_{pc} is reached, then it decreases beyond its peak value. Since the M_c/M_{pc} value is positive, the beam gets help from the column to carry the load and the column restrains the beam in the process. The restraint moment increases from zero to its maximum value and then decreases continuously to zero. When it becomes negative, the column will transfer the load to the beam and the beam will now
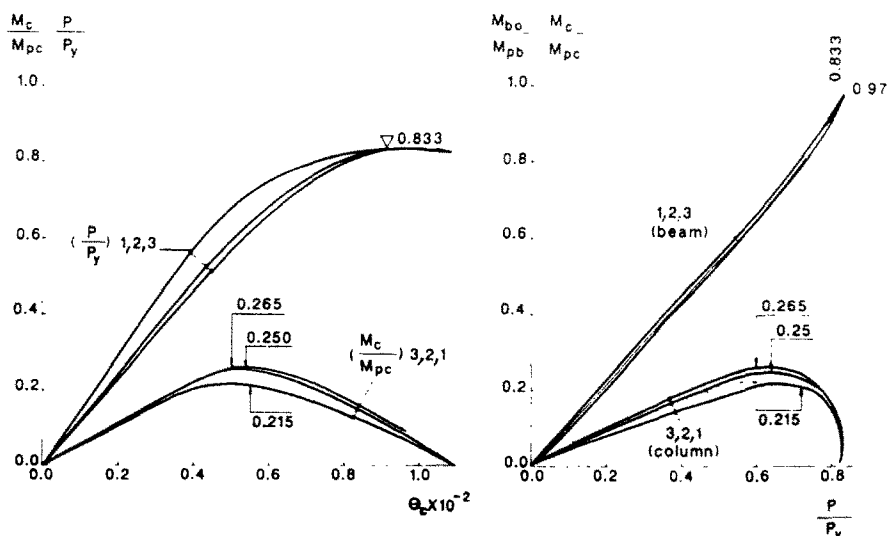
Fig. 9. The force, moment and rotation in the inelastic frame (A-II-1,2,3) with small eccentricity in columns ($M'_{pc}/M_{pc} = 0.220$ for $P/P_y = 0.833$ in column).

restrain the column, but this restraint happens to be in the descending branch of the curve, so it does not have really much practical significance.

The moment M_{bo} at the midspan of the beam increases as P/P_y increases. As the restraint provided by the columns to the beam decreases rapidly beyond the load $P/P_y = 0.7$, M_{bo} increases accordingly. When the column buckles, the corresponding M_{bo} value is $0.97 M_{bp}$. In the post-buckling range, the M_{bo} value increases continuously until a plastic hinge is formed in the midspan of the beam.

In this type of frame, failure will occur as the result of column buckling. At the buckling load $P/P_y = 0.833$ and M_c/M_{pc} is about 0.1 but the full plastic moment capacity for the column M'_{pc} at $P/P_y = 0.833$ is 0.220. Thus, there is no possible plastic hinge formation at the end of columns.

In the case of small eccentricity, the maximum moment M_r developed in the connection has never exceeded the maximum moment capacity of the connection. The connection behaves essentially as a linear elastic spring. As a result, the flexibility of the connection only affects the overall deformation of the frame but not its load-carrying capacity.

Figure 10 shows the behavior of Frame B with Load Pattern II and Connection Type 3, 2, and 1. In this case, it is almost identical to that of Frame A-II-3, 2, 1. The maximum load-carrying capacity ($P/P_y = 0.645$) is less than that of Frame A-II-3,2,1. This is because in Frame A, the relative stiffness ratio of the beam to the column is $G_b/G_c = 8.18$, but in Frame B, $G_b/G_c = 4.0$, the column is relatively stronger in Frame B than in Frame A, so the influence of column restraint to the beam is relatively greater. This will cause a reduction in the load-carrying capacity of the columns, and thus, will reduce the load-carrying capacity of the frame as a whole.

Figure 11 summarizes and compares the results of Frame A with Frame B with different flexible connections. The load-carrying capacity of the frames with hinges at the beam to column joints, A-II-0 or B-II-0 is found to be stronger or at least near to that of A-II-3,2,1 or B-II-3,2,1. Here, it appears that increasing the stiffness of the joint does not necessarily increase the load-carrying capacity of the frame. This is because in Frame A-II or Frame B-II, the load on the beam is relatively small compared with the load on the columns. The columns therefore control the load-carrying capacity of the frame. As a result, the restraint provided by the column to the beam through the rigidity of connections cannot help much to increase the load-carrying capacity of the frame. On the contrary, the rigidity of the connection introduces an eccentricity to the column and thus, results in a reduction in the load-carrying capacity of the frame. In Frames A-II-0 and B-II-0, the column is loaded concentrically, and thus the columns have a higher load-carrying capacity.
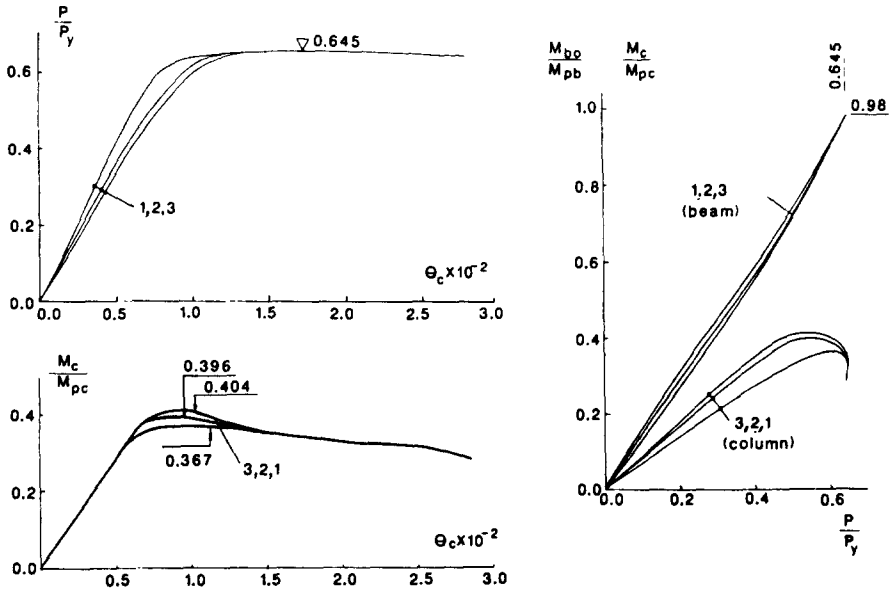
Fig. 10. The force, moment and rotation in the inelastic frame (B-II-1,2,3) with small eccentricity in columns ($M'_{pc}/M_{pc} = 0.419$ for $P/P_y = 0.645$ in column).

2P/3 2P/3	M_{bo}	M_c M_{bo}	M_c M_{bo}	M_c M_{bo}
2P/3L_b $\frac{A}{B}$ – II	$\frac{A}{B}$ – II –0	$\frac{A}{B}$ – II –1	$\frac{A}{B}$ – II –2	$\frac{A}{B}$ – II –3
$\frac{M_c}{M_{pc}}$ A	0	0.215	0.25	0.265
B	0	0.367	0.396	0.404
$\frac{M_{bo}}{M_{pb}}$ A	1	0.97	0.97	0.97
B	1	0.98	0.98	0.98
failure form	plastic hinge in beam	column buckling		
Loading Capacity A $\frac{W}{P_y} = \frac{2P}{P_y}$	1.697	1.666	1.666	1.666
B	1.171	1.29	1.29	1.29

Fig. 11. Failure of Frames A-II and B-II with small eccentricity in columns.

The load-carrying capacity of the centrally loaded columns shown in Fig. 12 is higher than that of the eccentrically loaded columns. Hence, the load-carrying capacity of the frame is controlled by the formation of a plastic hinge at the beam midspan.

6.3. Frame with medium eccentricity in columns

The behavior of frames with medium eccentricity in columns is illustrated in Figs 13–16 (Frames A-III and B-III). The failure of this type of frame is due to the buckling of the columns and the formation of a plastic hinge at the midspan of the beam.

For Frame A-III-3, the moment–rotation curves for the column and the beam as shown in Fig. 13 are calculated with $P/P_y = 0.1, 0.2, 0.3, 0.4, 0.5, 0.6, 0.61, 0.615, 0.616$ and 0.617. The curves for the beam appear linear when P/P_y is less than 0.5, so in this loading range, the beam is essentially elastic. When P/P_y exceeds 0.5, the curves for the beam become nonlinear and bend over rapidly to approach a horizontal line when θ_b is greater than, say, 1.5×10^{-2} rad. In this range, the beam is inelastic and a plastic hinge will form
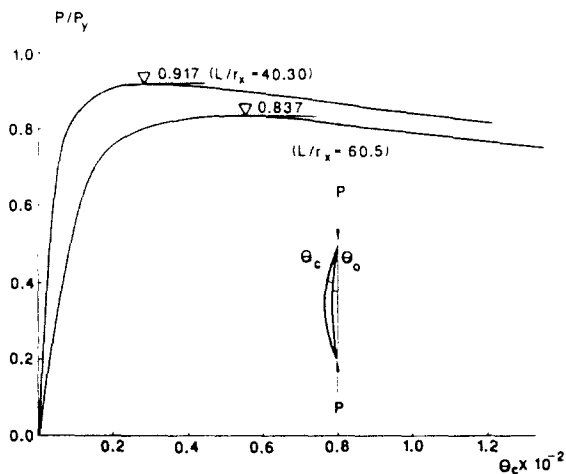
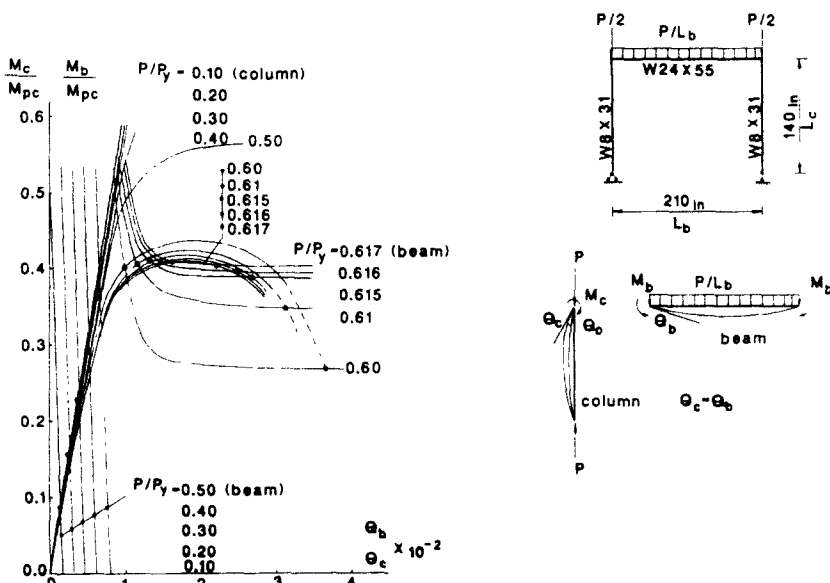Fig. 12. The curves of centrally loaded columns (W8 × 31).

Fig. 13. The (M/M_{pc})–θ curve of the inelastic rigid frame (A-III-3) with medium eccentricity in columns.
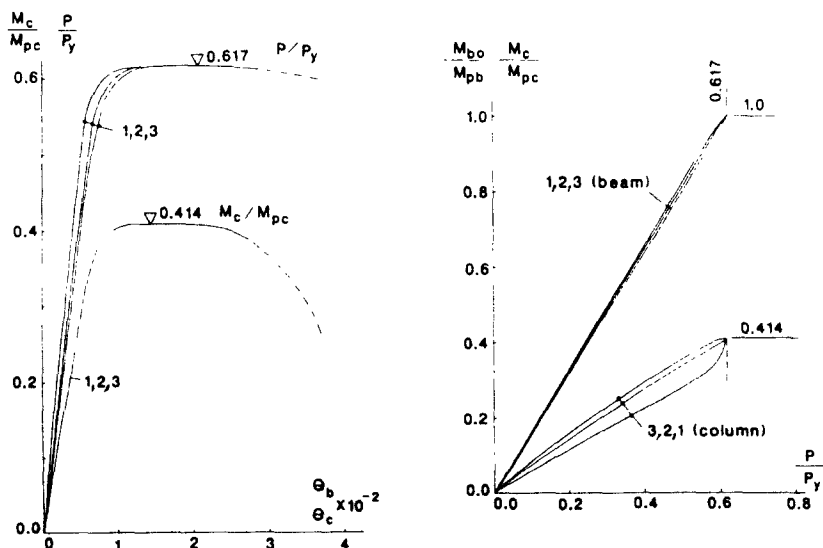

Fig. 14. The force, moment and rotation in the inelastic frame (A-III-1,2,3) with medium eccentricity in columns ($M'_{pc}/M_{pc} = 0.451$ for $P/P_y = 0.617$ in column).
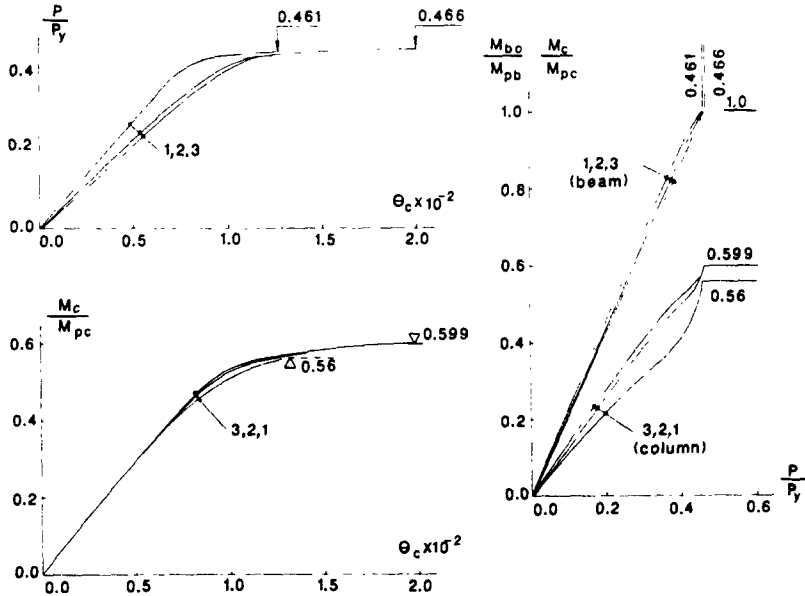
Fig. 15. The force, moment and rotation in the inelastic frame (B-III-1,2,3) with medium eccentricity in columns ($M'_{pc}/M_{pc} = 0.617$ for $P/P_y = 0.466$ in column).
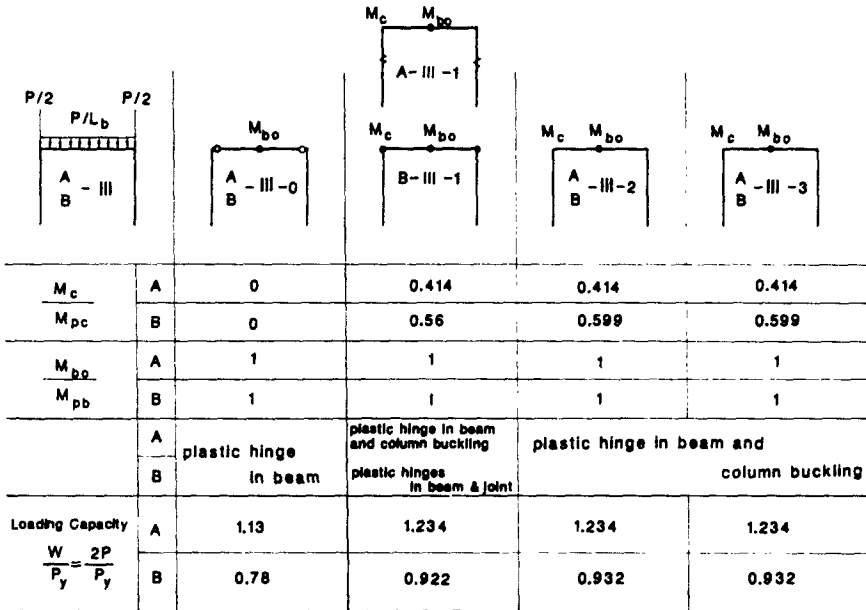

Fig. 16. Failure of Frames A-III and B-III with medium eccentricity in columns.

at the midspan of the beam for which the curve becomes horizontal. At load $P/P_y = 0.617$, the two columns buckle and the plastic hinge is formed simultaneously at the midspan of the beam. So, during the entire post-buckling range, there is a plastic hinge formed in the midspan of the beam.

During the entire loading and unloading process for Frames A-III and B-III (Figs 14 and 15) the beam transfers load to the column and correspondingly the column restrains the beam. The restraint moment for the beam (or the end moment carried by the column) is greater than that of Frames A-II and B-II. The moment will increase as P/P_y increases and the moment decreases only in or near the descending branch of the load–rotation curve (P/P_y) vs θ_c. (For Frame B-III, the descending branch of the curve is not shown.)

In Frames A-III and B-III, if the moment M_c does not exceed the connection limiting
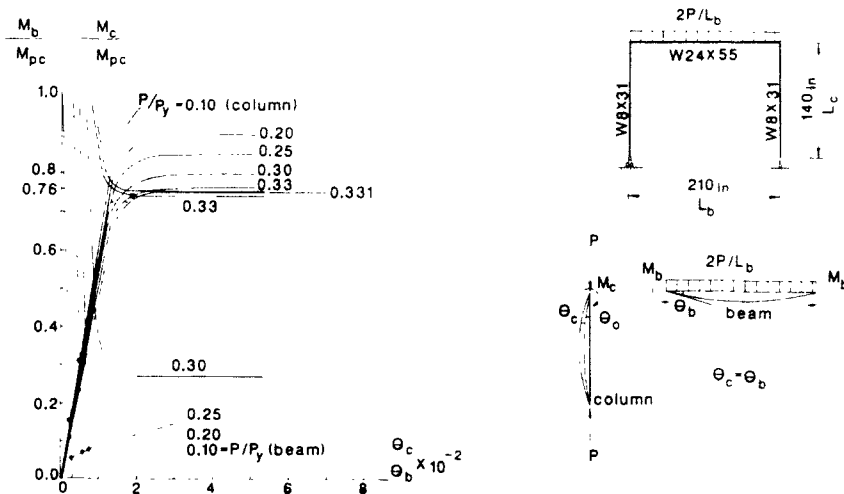
Fig. 17. The $M/M_{pc}-\theta$ curve in the inelastic rigid frame (A-IV-3) with large eccentricity in columns.
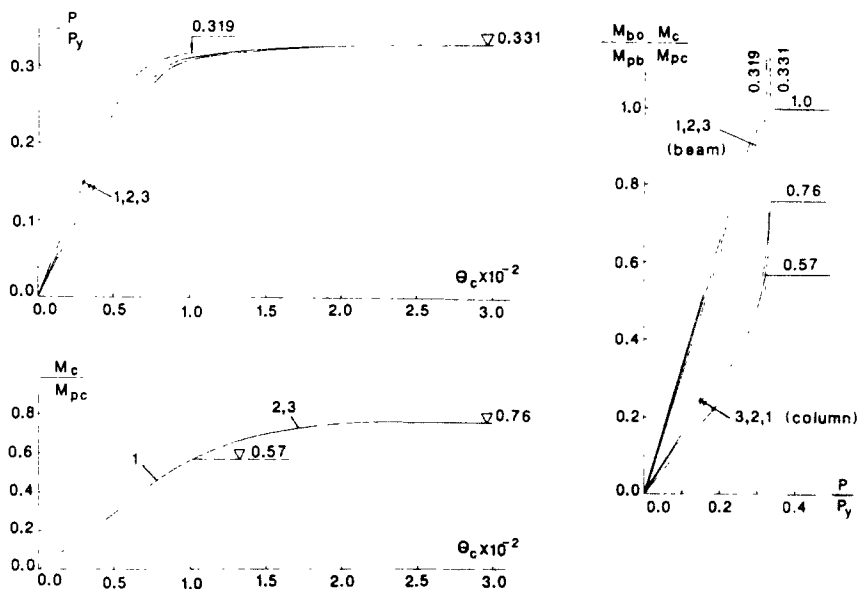

Fig. 18. The force, moment and rotation in the inelastic frame (A-IV-1,2,3) with large eccentricity in columns ($M'_{pc}/M_{pc} = 0.765$ for $P/P_y = 0.331$ in column).

moment, the flexibility of the connection will not affect the load-carrying capacity of the frame. For Frame B-III-1, the maximum moment M_c is $0.56M_{pc}$ which is very near the connection limiting moment. As a result, a plastic hinge is almost developed at the connection and another plastic hinge is formed at the midspan of the beam. The failure of the frame is due to the formation of a collapse mechanism.

Comparing with A-III-0 and B-III-0, the load-carrying capacity of Frames A-III-3,2,1 and B-III-3,2,1 is higher, since the rigidity of connection makes the column restrain the beam, so that the formation of a plastic hinge at the midspan of the beam is delayed.

6.4. Frame with large eccentricity in columns

The behavior of frames with large eccentrically loaded columns is shown in Figs 17–20 (Frames A-IV and B-IV). The failure of this type of frame is due to the formation of plastic hinges at the midspan of the beam as well as at the top of the columns or joints, so the frame forms a plastic failure mechanism.

For Frame A-IV-3, the moment–rotation curves for columns and beams as shown in
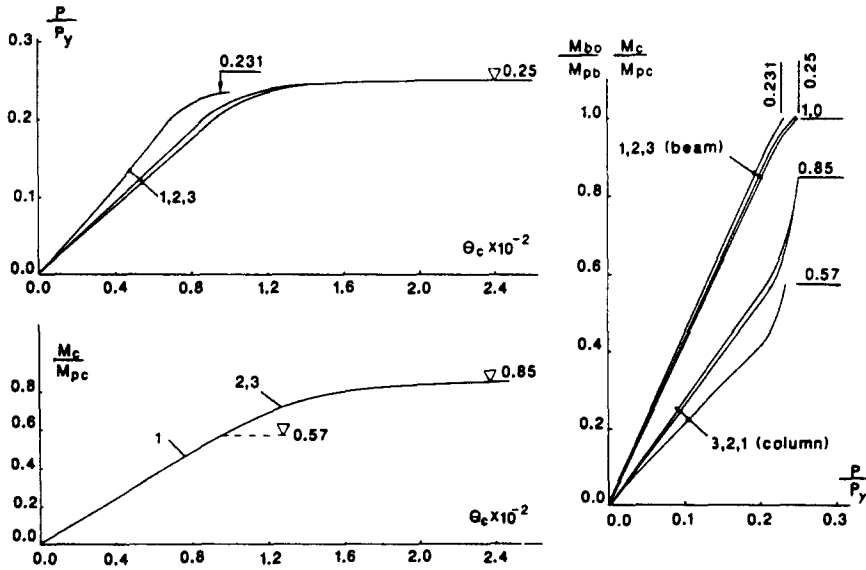
Fig. 19. The force, moment and rotation in the inelastic frame (B-IV-1,2,3) with large eccentricity in columns ($M'_{pc}/M_{pc} = 0.852$ for $P/P_y = 0.25$ in column).

2P/L_b		Mbo		Mc Mbo		Mc Mbo		Mc Mbo	
A/B - IV		A/B -IV-0		A/B - IV-1		A/B - IV-2		A/B - IV-3	
$\dfrac{M_c}{M_{pc}}$	A	0		0.57		0.76		0.76	
	B	0		0.57		0.85		0.85	
$\dfrac{M_{bo}}{M_{pb}}$	A	1		1		1		1	
	B	1		1		1		1	
failure form		plastic hinge in beam		plastic hinge in beam plastic hinge in joint		plastic hinges in beam and columns			
Loading Capacity	A	0.57		0.638		0.662		0.662	
$\dfrac{W}{P_y} = \dfrac{2P}{P_y}$	B	0.39		0.462		0.50		0.50	

Fig. 20. Failure of Frames A-IV and B-IV with large eccentricity in columns.

Fig. 17 are calculated with $P/P_y = 0.1$, 0.2, 0.25, 0.3, 0.33, 0.331. Both beam and column curves overlap along a horizontal line at $P/P_y = 0.331$. At this load, plastic hinges are formed on the top end of the columns and at the midspan of the beam. As a result, a failure mechanism for the frame is formed.

During the entire loading process for Frames A-IV and B-IV (Figs 18 and 19), the beam continues to transfer the load to columns and the columns restrain the beam. The moments M_c (or M_{bo} or M_r) in Frames A-IV and B-IV are greater than those in Frames A-III and B-III, since in the present case, the eccentricity is greater for the columns. As P/P_y increases, M_c/M_{pc} and M_{bo}/M_{pb} will increase too. When P/P_y is near the maximum value, the M_c/M_{pc} value increases rapidly until the full plastic moment capacity M'_{pc} for columns or the moment capacity $0.57 M_{pc}$ for Connection Type 1 is reached. The M_{bo}/M_{pb} value increases more slowly until the full plastic moment M_{bp} is reached.

For Frames A-IV-1 and B-IV-1, the columns provide restraint to the beam and this restraint decreases due to the flexibility of the connection. As a result, the value of M_{bo} increases rapidly. This leads to an early formation of the failure mechanism (plastic hinges at the connecting joint and at the midspan of the beam). Hence, the load-carrying capacity of the frame is lower than that of Frames A-IV-2,3 and B-IV-2,3 (Fig. 20).
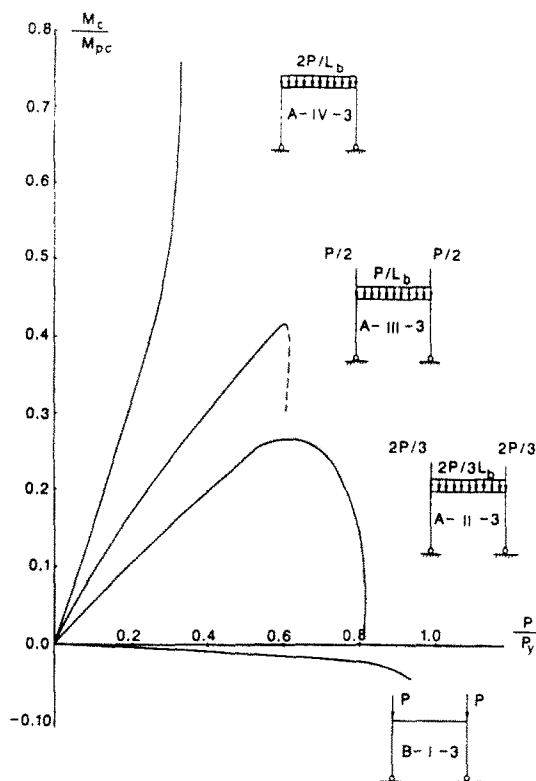
Fig. 21. Comparison of $M_c/M_{pc} \sim P/P_y$ curves of rigid Frames A and B with different load type

7. CONCLUSIONS

(1) In the inelastic analysis, in order to satisfy the equilibrium and compatibility conditions of a loaded frame at the joints, the beam and the columns in the frame must restrain each other (or to enhance the load-carrying capacity of the frame). In some cases, the column restrains the beam and the beam transfers the load to the column and in other cases, they play opposite roles. This interacting role depends on the geometry and load patterns of the frame and the moment–rotation characteristics of the joint used.

When the column restrains the beam, the end moment of the beam is in an opposite direction to its end rotation. The load-carrying capacity of the beam will therefore be enhanced compared with that of a pin-ended beam, but the load-carrying capacity of the columns will be lower than that of a pin-ended column with the centrally loaded condition. Depending on the load patterns in the beam and in the column, the failure mode of the frame can be quite different. The possible failure modes include the plastic collapse mechanism, column buckling, and column buckling with a plastic hinge in the midspan of the beam.

(2) In the structural analysis for columns with end eccentricity, two loading procedures are usually taken: (a) the end moment and axial force are increased proportionally; and (b) either the end moment or the axial force is kept constant, while the other is increased to failure. For a column in an actual frame, neither loading Path (a) nor Path (b) is correct. As the axial force is increased, it is possible that the moment at the end of a column in a frame increases or decreases and the direction of the moment can be either positive (transferring beam moment to column) or negative (transferring column moment to beam). Figure 21 illustrates this comparison of the M_c/M_{pc} and P/P_y curve of Frames A and B for different types of loading patterns.

(3) If the moment capacity of a connection is greater than the end moment of the column, the joint flexibility will not reduce the load-carrying capacity of the frame, compared with that for a frame with rigid joints. However, the joint flexibility will increase the overall deformations of the frame.

Comparing the frame with pinned connections at the joints, rigidity of connections can enhance the load-carrying capacity of the frame. But in the cases when the load on the beam is small compared with the load on the columns, the rigidity of connection will reduce the load-carrying capacity of the frame.

(4) To develop design rules in the limit states design of frames with flexible joints, further study of the inelastic analysis and behavior of such frames is needed.

REFERENCES

1. American Institute of Steel Construction, Load and resistance factor design specification for structural steel buildings, Chicago, Illinois (November 1986).
2. E. M. Lui, Effects of connection flexibility and panel zone deformation on behavior of plane steel frames. Ph.D. dissertation, Department of Civil Engineering, Purdue University, West Lafayette, IN 47907 (May 1985).
3. M. J. Frey and G. A. Morris, Analysis of flexibly connected steel frames. *Can. J. Civil Engrs* **2**, 280–291 (1975).
4. S. W. Jones, P. A. Kirby and D. A. Nethercot, Columns with semi-rigid joints. *J. Struct. Div. ASCE* **108** (ST2), 361–372 (February 1982).
5. S. P. Zhou and W. F. Chen, On C_m factor in LRFD. *J. Struct. Engng ASCE* (1987), in press.
6. W. F. Chen and T. Atsuta, *Theory of Beam-Columns*, Vol. 1. McGraw-Hill, New York (1977).
7. T. V. Galambos, *Structural Members and Frames*. Prentice-Hall, Englewood Cliffs, New Jersey (1968).